Contents List available at VOLKSON PRESS

New Materials and Intelligent Manufacturing (NMIM)

DOI : http://doi.org/10.26480/icnmim.01.2018.333.335

Journal Homepage: https://topicsonchemeng.org.my/

ISBN: 978-1-948012-12-6

PREPARATION OF MAGNETIC ZR-PILLARED BENTONITE AND ITS APPLICATION IN CONGO RED REMOVAL

Lian Li, Li Lv Jin, Yi Liu Yi, Min Ren Zhong, Yuan Ma Xian, Hong Lou Da Wei*

Department of Analytical Chemistry, Jilin Institute of Chemical Technology, Jilin 132022, P. R. China
Corresponding Autho: dwlou@hotmail.com (D.W. Lou)

ARTICLE DETAILS

Article History:

Received 26 June 2018
Accepted 2 July 2018
Available online 1 August 2018

ABSTRACT

The magnetic bentonite material (Zr-B-Fe_3O_4) was prepared by a solvothermal reaction. The received Zr-B-Fe_3O_4 had the advantage of pillared bentonite and magnetic Fe_3O_4. It can be separated easily under an external magnetic field, due to the formation of Fe_3O_4 on the surface of bentonite. SEM image indicated that there were a number of mesoporous and stripped slice layers. Fe_3O_4 nanoparticles with a diameter of ~150 nm dispersed uniformly on the bentonite surface. Furthermore, Zr-B-Fe_3O_4 was used to remove Congo red dye in solution. The results showed that Zr-B-Fe_3O_4 could be employed as a low-cost material for removal of Congo red from aqueous solutions effectively and conveniently.

KEYWORDS

Magnetic, Bentonite, Adsorption, Pillared.

1. INTRODUCTION

Bentonite is a non-metallic mineral containing montmorillonite as the main mineral component. It is consisted of silica (SiO_2), aluminum oxide (Al_2O_3) and water. There are certain cations (such as Na^+, Ca^{2+}, K^+, Mg^{2+}, etc.) between the layer of bentonite, which are easily exchanged by other cations [1-3]. Bentonite materials can be used to remove many pollutants in water, such as heavy metal ions, organic pollutants, and dyes [4-10]. However, it is difficult to separate from solution which limits the practical application of bentonite in waste water treatment.

Magnetic nanoparticles is an important class of nanomaterials [11-14]. Among them, Fe_3O_4 nanoparticles is one of the most widely used ferrite magnetic nanomaterials. In order to improve the adsorption capacity and reduce the preparation cost of magnetic materials, scholar have exploited a series of modification methods [15-20]. It is worth noting that, Wu prepared the magnetic GMZ bentonite composite by a simple co-precipitation method [21]. The received magnetic material kept the physical properties of natural bentonite and showed a good adsorption capacity for rare metal elements in water. In order to improve the magnetism and adsorption capacity of the magnetic composites, we prepare the magnetic Zr-pillared bentonite by a simple one pot solvothermal method.

2. EXPERIMENTAL PART

2.1 Materials and reagents

All chemical reagents were of analytical grade and used as received. Distilled water was used for all synthesis and treatment processes. Congo red dye was purchased from Alfa Aesar Co., Ltd. The Congo red solution of 1000 mg·L^{-1} was prepared by dissolving Congo red in distilled water. The dye solutions of different concentrations used in the experiments were diluted with the stock solution. $FeCl_3·6H_2O$, ethylene glycol, polyethylene glycol, and anhydrous sodium acetate were purchased from Tianjin Damao Chemical Reagent Manufacturing.

2.2 Instrumentation

The morphology of Zr-B-Fe_3O_4 was observed by H-7500 transmission electron microscope (Hitachi, Japan). The functional groups were characterized by the Vertex 80V FT-IR infrared spectrometer (Bruker, Germany). The N_2 adsorption-desorption isothermal curve of Zr-B-Fe_3O_4 was measured by using an ASAP 2000M automatic micropore analyzer (Micromeritics, USA). The magnetic property of Zr-B-Fe_3O_4 was tested by Quantum Design's Superconducting Quantum Interference (SQUID) vibrating magnetometer (MPMS XL-5, USA) . The absorbance of Congo red solution was measured by Shimadzu UV-3600 ultraviolet-visible spectrophotometer (497 nm).

2.3 Preparation of Zr-B-Fe_3O_4

2.3.1 Preparation of Zr-pillared Bentonite (Zr-B)

0.1 mol/L $ZrOCl_2$ solution was dropwised added to 2% calcium ion-exchanged bentonite until the Zr^{4+}/bentonite ratio was 3 mmol·g^{-1} [22]. The mixture was stirred at 65°C for 2 h, aged for 4 h, and washed with distilled water. After dry at 110 °C, it was calcined at 300 °C for 3 h.

2.3.2 Preparation of magnetic bentonite (Zr-B-Fe_3O_4)

2.0 g pillared bentonite, 1.35 g $FeCl_3.6H_2O$, 3.60 g of NaAc and 1.00 g of polyethylene glycol were dissolved in 40 mL of ethylene glycol. The mixture was stirred to form a homogeneous yellow-brown solution, and then heated at 190 °C for 8 h. After separation by a magnet, the received magnetic composite was washed with distilled water and ethanol and placed in a vacuum drying oven at 60 °C for 6 h.

2.3.3 Congo red adsorption

The single factor experiment method was used to determine the best conditions for dye adsorption. A certain amount of adsorbent was added to the 50 mL Congo red dye solution. After shaken for a certain time, the dye-loaded adsorbent was separated by an external magnetic field; the solution was measured at 497 nm using a spectrophotometer. The experiment parameters, such as equilibrium time, temperature, and

concentration were investigate in this study [23].

3. RESULTS AND DISCUSSION

3.1 Properties of Zr-B-Fe_3O_4

SEM was used to confirm the morphological characteristics of Zr-B-Fe_3O_4. As show in Fig.1, the spherical shape Fe_3O_4 nanoparticles with a diameter of ~150 nm, uniformly disperses on the surface of bentonite.

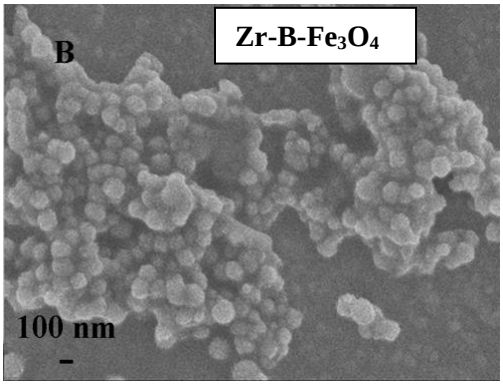

Figure 1: SEM image of Zr-B-Fe_3O_4 magnetic material

As shown in Fig.2, the N_2 sorption-desorption isotherm belongs to IV type sorption isotherm in the IUPAC classification. The calculated BET specific surface area is 109.59 $m^2.g^{-1}$. Compared with the nature bentonite, the specific surface area increases obviously, indicating inorganic pillared agent entrance the space of bentonite layers.

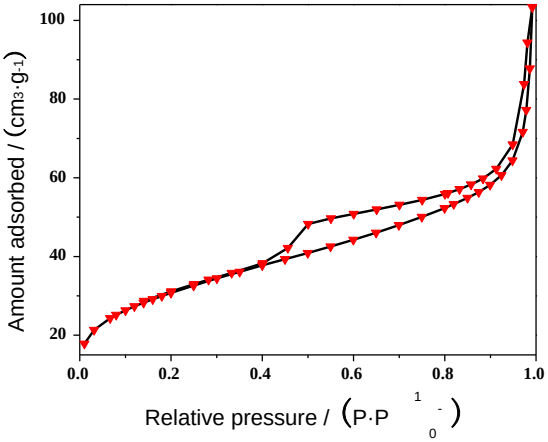

Figure 2: Adsorption and desorption isotherms of N_2 by Zr-B-Fe3O4

Fig.3 shows the hysteresis loop of Zr-B-Fe_3O_4 measured at room temperature. The saturation magnetization of Zr-B-Fe_3O_4 is 37.5 emu.g^{-1}. Fig.3 also indicates that the prepared magnetic bentonite material has superparamagnetism, which is favorable for its easy dispersion in aqueous solution and magnetic separation after adsorption.

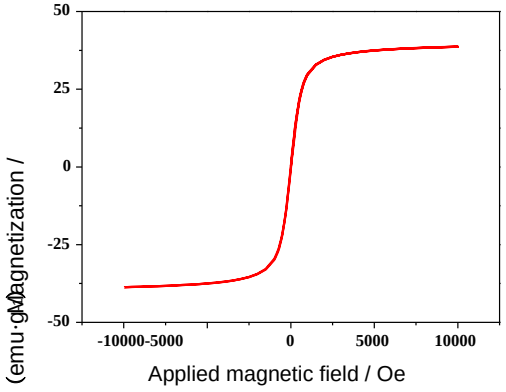

Figure 3: Hysteresis loop of the Zr-B-Fe_3O_4 magnetic material

3.2 Effect of temperature on the amount of adsorption

0.05 g Zr-B-Fe_3O_4 was placed in a 30 $mg.L^{-1}$ dye solution and shaken at different temperatures (20-50℃) for a certain time. The effect of temperature on the dye uptake is shown in Fig.4. The dye uptake increases significantly during the first 60 min. Then, the dye uptake decelerates over time and the adsorption nearly finished within 180 min. Furthermore, the dye uptake were significantly increased with temperature.

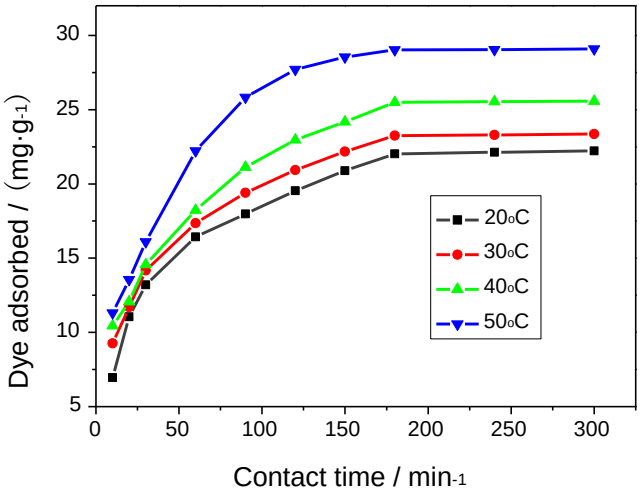

Figure 4: The influence of temperature on the adsorption

3.3 Adsorption kinetics

0.05g of Zr-B-Fe_3O_4 was added into 50 mL of Congo red solution with the concentrations of 40, 60, and 80 $mg{\cdot}L^{-1}$, respectively. After incubation at a given time, 5 mL solution was taken from the vessel for absorbance determination. The amount of dye adsorbed by Zr-B-Fe_3O_4 increases with the increase of initial concentration; when the dye concentration increased from 40 $mg{\cdot}L^{-1}$ to 80 $mg{\cdot}L^{-1}$, the dye uptake increases from 30.85 $mg{\cdot}g^{-1}$ to 42.00 $mg{\cdot}g^{-1}$. The pseudo-first-order kinetics and pseudo-second-order kinetic models were used to fit the adsorption data. Fig.5 indicates that the experimental data fit well to the pseudo-second-order model with high correlation coefficients between 0.9985 and 0.9999 (R^2 > 0.999). The adsorption data is also fitted by a intra-particle diffusion model. The correlation coefficient is between 0.7076 and 0.9366, indicating that the diffusion between particles is not the rate determination step.

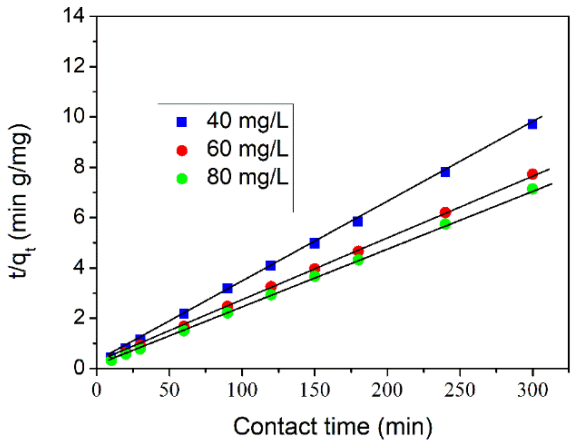

Figure 5: The influence of concentration on the absorption of dye

3.4 Isothermal studies

Langmuir and Freundlich isotherms were used to evaluate the adsorption capacity of the adsorbent. The relevant parameters qmax, b, kf, rL_2, and rF_2 are listed in Table 1. From the correlation coefficients listed in Table 1, the

Langmuir modle fits the adsorption data better than the Freundlich modle. The maximum adsorption capacity (q_{max}) of Zr-B-Fe_3O_4 calculated from the Langmuir isotherm equation is 63.29 mg/g.

Table 1: Adsorption isotherm parameters of adsorbed Congo red on Zr-B-Fe_3O_4

Langmuir			*Freundich*		
q_{max} /(mg·g^{-1})	b/(L·mg^{-1})	r_L^2	k_f	n	r_F^2
63.29	0.0589	0.90	6.2933	1.789	0.89

4. CONCLUSION

In this study, the Zr-B-Fe_3O_4 magnetic adsorbent was prepared by a one pot solvothermal synthesis method. Compared with the magnetic bentonite materials prepared by co-precipitation method, Zr-B-Fe_3O_4 prepared by solvothermal synthesis method had more regular morphology and stronger magnetic properties.

The received magnetic adsorbent was used to remove Congo red dye from solution. The adsorption of Congo red on Zr-B-Fe_3O_4 was fast; the adsorption equilibrium can be reached within 180 min. The adsorption process fit the pseudo second-order kinetic equation and Langmuir adsorption model well. The received Zr-B-Fe_3O_4 magnetic adsorbent is expected to be a promising candidate for dye discoloration because of its cost-effective, facile, and excellent adsorption capacity.

ACKNOWLEGEDMENT

The present work is supported by the projects of National Natural Science Foundation of China (21605056), Natural Science Foundation of Jilin Province (20180101292JC, 20170520032JH), and the Science Foundation for Distinguished Young Scholars of Jilin City (No. 20166028). Financial support from the Key Laboratory of Fine Chemicals of Jilin Province is also acknowledged.

REFERENCES

[1] Dernane, C., Zazoua, A., Kazane, I., Jaffrezic-Renault, N. 2013. Cadmium-sensitive electrode based on tetracetone derivatives of p-tert-butylcalix [8] arene. Materials Science and Engineering C Materials for Biological Applications, 33 (7), 36-38.

[2] Alzaydien, A.S. 2009. Adsorption of methylene blue from aqueous solution onto a low-cost natural jordanian tripoli. American Journal of Environmental Sciences, 5 (3), 1047-1058.

[3] Thaldiri, N.H., Hanafiah, M.M., Halim, A.A. 2017. Effect of modified micro-sand, poly-aluminium chloride and cationic polymer on coagulation-flocculation process of landfill leachate. Environment Ecosystem Science, 1 (1), 17-19.

[4] Sen, T.K., Gomez, D. 2011. Adsorption of zinc (zn 2+) from aqueous solution on natural bentonite. Desalination, 267 (2), 286-294.

[5] Lian, L., Guo, L., Guo, C. 2009. Adsorption of congo red from aqueous solutions onto ca-bentonite. Journal of Hazardous Materials, 161 (1), 126-31.

[6] Vazdani, S., Sabzghabaei, G.R., Dashti, S., Cheraghi, M., Alizadeh, R., Hemmati, A. 2017. Fmea Techniques Used in Environmental Risk Assessment. Environment Ecosystem Science, 1 (2), 16-18.

[7] Omar, H., Arida, H., Daifullah, A. 2009. Adsorption of 60co radionuclides from aqueous solution by raw and modified bentonite. Applied Clay Science, 44 (1–2), 21-26.

[8] Melero, J.A., Bautista, L.F., Iglesias, J., Morales, G., Sánchez-Vazquez, R. 2014. Production of biodiesel from waste cooking oil in a continuous packed bed reactor with an agglomerated zr-sba-15/bentonite catalyst. Applied Catalysis B Environmental, 145 (1), 197-204.

[9] Ping, Jing, Meifang, Ping, Zhao, Xiaoyan. 2013. Adsorption of 2-mercaptobenzothiazole from aqueous solution by organo-bentonite. Journal of Environmental Science, 25 (6), 1139-1144.

[10] Yang, Z.Q., Xiao, O., Chen, B., Zhang, L.X., Zhang, H.G., Niu, X.J., Zhou, S.Q. 2013. Chem. Eng. J., 223, 31. doi. org/10.1016/j.cej. 2013.02.085

[11] Gao, M.X., Deng, C.H., Fan, Z.Q., Yao, N., Xu, X.Q., Yang, P.Y., Zhang, X.G. 2007. 3, 1714. doi: 10.1002/smll. 200700149

[12] Liu, X.C., Dang, Y.Q., Wu, Y.Q. 2010. A convenient method for the preparation of surface-aminated superparamagnetic fe3o4 nanoparticles. Journal of Physical Chemistry, 26 (3), 789-794.

[13] Xia, J., Song, L.J., Dang, Z., Shao, Z.C. 2013. Polyethylene Glycol/Fe3O4 Nanoparticle Composite Materials: Structure, Physical Properties and Application. Acta Physico-Chimica Sinica, 29 (7), 1524-1533.

[14] Ma, Z., Meng, F.B., Zhao, R., Zhan, Y.Q., Zhong, J.C., Liu, X.B.J. 2012. Magn. Mater., 324, 1365. doi. org/10.1016/j.jmmm. 2011.11.040

[15] Murakami, M., Matsuda, T. 2011. Metal-catalysed cleavage of carbon-carbon bonds. Chemical Communications, 47 (4), 1100-1105.

[16] Wu, C., Zhuang, Q., Wu, Y., Tian, L., Cui, Y., Zhang, X. 2013. Facile synthesis of fe3o4 hollow spheres/carbon nanotubes composites for lithium ion batteries with high-rate capacity and improved long-cycle performance. Materials Letters, 113 (24), 1-4.

[17] Li, S.K., Huang, F.Z., Wang, Y., Shen, Y.H., Qiu, L.G., Xie, A.J., Xu, S.J.J. 2011. Magnetic Fe3O4@C@Cu2O composites with bean-like core/shell nanostructures: Synthesis, properties and application in recyclable photocatalytic degradation of dye pollutants. Journal of Materials Chemistry, 21, 7459. doi. 10.1039/C0JM04569A

[18] Heidari, H., Razmi, H., Jouyban, A. 2012. Preparation and characterization of ceramic/carbon coated fe 3 o 4, magnetic nanoparticle nanocomposite as a solid-phase microextraction adsorbent. Journal of Chromatography A, 1245 (1245), 1-7.

[19] Zhou, L.M., Shang, C., Liu, Z.R. 2011. Kinetics and Thermodynamics of Adsorption of Chlorophenols onto β-Cyclodextrin Modified Chitosan. Acta Physico-Chimica Sinica, 28 (7), 1615-1622.

[20] Chen, H., Lu, X., Deng, C., Yan, X. 2009. Facile synthesis of uniform microspheres composed of a magnetite core and copper silicate nanotube shell for removal of microcystins in water. Journal of Physical Chemistry C, 113 (50), 21068-21073.

[21] Chen, Y.G., Zhu, B.H., Wu, D.B., Wang, Q.G., Yang, Y.H., Ye, W.M., Guo, J.F. 2012. Eu (III) adsorption using di(2-thylhexly) phosphoric acid-immobilized magnetic GMZ bentonite. Chemical Engineering Journal, 181, 387-396. doi. org/10.1016/j.cej. 2011.11.100

[22] Anirudhan, T.S., Bringle, C.D., Radhakrishnan, P.G. Heavy metal interactions with phosphatic clay: Kinetic and equilibrium studies. Chemical Engineering Journal, 200-202, 149-157. doi.org/10.1016/j.cej.2012.06.024

[23] Bouberka, Z., Khenifi, A., Benderdouche, N., Derriche, Z. 2006. Removal of supranol yellow 4gl by adsorption onto cr-intercalated montmorillonite. Journal of Hazardous Materials, 133 (1–3), 154-161.